

# Assignment 3

## Paul Trapping of Atoms

Andrea Turci

February 7, 2024

### 1 Question 1

Let's consider a free particle in a one dimensional geometry subject to a time-dependent harmonic potential of the form:

$$\hat{W}(t) = \frac{1}{2}m\omega_0^2\hat{x}^2\cos(\omega t) \quad (1)$$

This potential is unbounded from below for half period, meaning that the cosine provides a positive damping factor when  $-\frac{\pi}{2} + 2\pi n < \omega t < \frac{\pi}{2} + 2\pi n$ : in this range the harmonic potential has a minimum (always in  $x = 0$ ), otherwise the parabola faces down and it has a maximum, which leads to instability.

However, it is possible to prove that a particle that feels this potential for large oscillation frequencies  $\omega$  is indeed trapped (the reason is that the potential flips so rapidly that there isn't time for the instability to have an effect on the particle). Indeed, let's consider the correspondent Hamiltonian as:

$$\begin{aligned} \hat{H}(t) &= \hat{H}_0 + \hat{W}(t) = \frac{p^2}{2m} + \frac{1}{2}m\omega_0^2\hat{x}^2\cos(\omega t) \\ &= \hat{H}_0 + \frac{m\omega_0^2\hat{x}^2}{4} (e^{i\omega t} + e^{-i\omega t}) \\ &= \hat{H}_0 + e^{i\omega t}\hat{V} + e^{-i\omega t}\hat{V}^\dagger \end{aligned}$$

where

$$\hat{V} = \hat{V}^\dagger = \frac{m\omega_0^2\hat{x}^2}{4}$$

The drive of the system is obviously time-periodic, since  $\hat{W}(t) = \hat{W}(t + T)$  with  $T = \frac{2\pi}{\omega}$ , and it is also monochromatic, so we have only one frequency. Thus, assuming as required an high-frequency regime ( $\omega \gg \|\hat{H}_0\|/\hbar$  and  $\omega \gg \omega_0$ ), it is possible to derive the effective time-independent Hamiltonian  $\hat{H}_{eff}$  using the high-frequency expansion formula; we stop the expansion up to the second order in  $o(1/\omega^2)$ :

$$H_{eff} = H_0 + \frac{1}{\hbar\omega}[V, V^\dagger] + \frac{1}{2(\hbar\omega)^2} \left( [[V, H_0], V^\dagger] + [[V^\dagger, H_0], V] \right) + O\left(\frac{1}{\omega^3}\right) \quad (2)$$

Since  $\hat{V}$  is hermitian the expression simplifies as:

$$H_{eff} = H_0 + \frac{1}{(\hbar\omega)^2} [[V, H_0], V] + O\left(\frac{1}{\omega^3}\right) \quad (3)$$

Let's now proceed with the computation of the commutators:

$$\begin{aligned} [\hat{V}, \hat{H}_0] &= \left[ \frac{m\omega_0^2}{4} \hat{x}^2, \frac{\hat{p}^2}{2m} \right] = \frac{\omega_0^2}{8} [\hat{x}^2, \hat{p}^2] = \frac{\omega_0^2 i\hbar}{4} (\hat{x}\hat{p} + \hat{p}\hat{x}) \\ [[V, H_0], V] &= \left[ \frac{i\hbar\omega_0^2}{4} (\hat{x}\hat{p} + \hat{p}\hat{x}), \frac{m\omega_0^2 \hat{x}^2}{4} \right] = \frac{i\hbar m\omega_0^4}{16} ([\hat{x}\hat{p}, \hat{x}^2] + [\hat{p}\hat{x}, \hat{x}^2]) \\ &= \frac{i\hbar m\omega_0^4}{16} (-4i\hbar \hat{x}^2) = \frac{m\omega_0^4 \hbar^2}{4} \hat{x}^2 \end{aligned}$$

where  $[\hat{x}^2, \hat{p}^2]$  and  $([\hat{x}\hat{p}, \hat{x}^2] + [\hat{p}\hat{x}, \hat{x}^2])$  are calculated using the rules derived in Appendix A.1. The following effective time-independent Hamiltonian is the result obtained:

$$\hat{H}_{eff} = \frac{\hat{p}^2}{2m} + \frac{m\omega_0^4 \hbar^2}{4\hbar^2 \omega^2} \hat{x}^2 = \frac{\hat{p}^2}{2m} + \frac{m\omega_0^2}{4} \left( \frac{\omega_0}{\omega} \right)^2 \hat{x}^2 \quad (4)$$

which indeed describes a particle under a harmonic potential.

## 2 Question 2

Let's now consider an optical lattice in the tight-binding regime, described by the following Hamiltonian:

$$\hat{H}(t) = \hat{H}_0 + \hat{W}(t) = -J \sum_i (|i+1\rangle \langle i| + |i\rangle \langle i+1|) + V \cos(\omega t) \sum_i i^2 |i\rangle \langle i| \quad (5)$$

where  $i \in [-N, N]$  and  $N$  is an integer such that the lattice has  $2N + 1$  sites. As it is possible to see, there is a time-independent kinetic component  $\hat{H}_0$  which describes the tunneling of particles between neighbours sites in the tight binding regime via the tunnelling coefficient  $J$ ; but there is also a potential part  $\hat{W}(t)$ , time dependent and monochromatic, that has a quadratic dependency on the number of the site in the lattice. Thus, we can approach this Hamiltonian as the discretization over the sites of the lattice of the Hamiltonian in Question 1.

Considering again the high-frequency regime with  $\omega \gg J, V$ , let's derive the effective Hamiltonian using Eq.(3), with:

$$\hat{H}_0 = -J \sum_i (|i+1\rangle \langle i| + |i\rangle \langle i+1|) \quad \text{and} \quad \hat{V} = \frac{V}{2} \sum_i i^2 |i\rangle \langle i|$$

The commutators become:

$$\begin{aligned}
[\hat{V}, \hat{H}_0] &= \frac{V}{2} \sum_i i^2 |i\rangle \langle i| \cdot \left( -J \sum_j (|j+1\rangle \langle j| + |j\rangle \langle j+1|) \right) + \\
&\quad - \left( -J \sum_i (|i+1\rangle \langle i| + |i\rangle \langle i+1|) \right) \cdot \frac{V}{2} \sum_j j^2 |j\rangle \langle j| = \\
&= -\frac{JV}{2} \sum_{i,j} \left( i^2 |i\rangle \underbrace{\langle i|j+1\rangle}_{\delta_{i,j+1}} \langle j| + i^2 |i\rangle \underbrace{\langle i|j\rangle}_{\delta_{i,j}} \langle j+1| \right) + \\
&\quad + \frac{JV}{2} \sum_{i,j} \left( j^2 |i+1\rangle \underbrace{\langle i|j\rangle}_{\delta_{i,j}} \langle j| + j^2 |i\rangle \underbrace{\langle i+1|j\rangle}_{\delta_{i+1,j}} \langle j| \right) = \\
&= -\frac{JV}{2} \left( \sum_i (i+1)^2 |i+1\rangle \langle i| + \sum_i i^2 |i\rangle \langle i+1| \right) + \\
&\quad + \frac{JV}{2} \left( \sum_i i^2 |i+1\rangle \langle i| + \sum_i (i+1)^2 |i\rangle \langle i+1| \right) = \\
&= -\frac{JV}{2} \sum_i ((2i+1) |i+1\rangle \langle i| - (2i+1) |i\rangle \langle i+1|) \\
\\
[[\hat{V}, \hat{H}_0], \hat{V}] &= -\frac{JV^2}{4} \left( \sum_i (2i+1) i^2 |i+1\rangle \langle i| - \sum_i (2i+1) (i+1)^2 |i\rangle \langle i+1| \right) + \\
&\quad + \frac{JV^2}{4} \left( \sum_i (i+1)^2 (2i+1) |i+1\rangle \langle i| - \sum_i i^2 (2i+1) |i\rangle \langle i+1| \right) = \\
&= \frac{JV^2}{4} \sum_i (2i+1)^2 (|i+1\rangle \langle i| + |i\rangle \langle i+1|)
\end{aligned}$$

Therefore, using natural units ( $\hbar = 1$ ), the effective Hamiltonian becomes:

$$\hat{H}_{eff} = \sum_i \left( -J + \frac{JV^2}{4\omega^2} (2i+1)^2 \right) (|i+1\rangle \langle i| + |i\rangle \langle i+1|) \quad (6)$$

We obtained an effective Hamiltonian with no diagonal elements; we have only kinetic components, so we can say that the hopping coefficient is changed and now it's space-dependent:

$$J' = J \left( 1 - \frac{V^2}{4\omega^2} (2i+1)^2 \right)$$

### 3 Question 3

Before answering this question and the following, it is safer to test numerically the behaviours of both the effective Hamiltonian of Eq.(6) and the time-dependent Hamiltonian of Eq.(5), in order to check if the calculations are correct.

In particular our goal is to study the time evolution of a wave function both in the high frequency and in the low-frequency regimes using the two Hamiltonians and prove that they are equivalent in the high frequency regime. We expect indeed that in the high-frequency regime

the secular motion is the dominant behaviour for  $\hat{H}(t)$ , which is the surviving term in the effective Hamiltonian  $\hat{H}_{eff}(t)$  (according to Eq.(2)), since the micromotion effect is expected to be negligible. On the other hand, while lowering the frequency, the micromotion becomes more and more important in  $\hat{H}(t)$  and thus in the time evolution of  $\hat{H}(t)$  we expect a lot of fluctuations, which are not present in  $\hat{H}_{eff}(t)$ .

The simulation is made considering a 5-sites lattice ( $N = 2$ ), that should be enough to display whether or not the agreement between the two time evolutions emerges in the high-frequency regime. A wave function is initialized in the middle of the lattice at the initial time:  $|\psi_0\rangle = |0\rangle$ . For the time-dependent Hamiltonian the time evolution operator is:

$$\hat{U}(t; 0) = \mathcal{T}exp\left(-\frac{i}{\hbar} \int_0^t H(t') dt'\right) \quad (7)$$

while for the effective Hamiltonian it reads as:

$$\hat{U}(t; 0) = e^{-\frac{i}{\hbar} H_{eff} t} \quad (8)$$

The simulation evolves the initial wave function over time, and afterwards we look at the probabilities of finding the evolved wave function in the sites of the lattice: given  $c_n(t)$  the amplitude in the  $n$ -th site, the correspondent probability is thus  $|c_n(t)|^2$ .

### High-frequency regime :

The following parameters have been used:

- $J = 0.5$
- $V = 1$
- $\omega = 7$

Using  $\hat{H}(t)$ , in Figure 1 the probabilities of measuring the particle in site 0, 1 and 2 are depicted over time, while Figure 2 is a schematic of the correspondent amplitudes. Instead, the analogous plots representing the probabilities and the amplitudes of the wave function using  $\hat{H}_{eff}$  are depicted in Figure 3 and 4 respectively.

As it can be seen, the behaviours are quite similar in the two regimes, as the secular motion provides the leading effect in  $\hat{H}(t)$ , even though some little wiggles due to the micromotion dynamics are still present.

### Low-frequency regime :

The following parameters have been used:

- $J = 0.5$
- $V = 1$
- $\omega = 1.2$

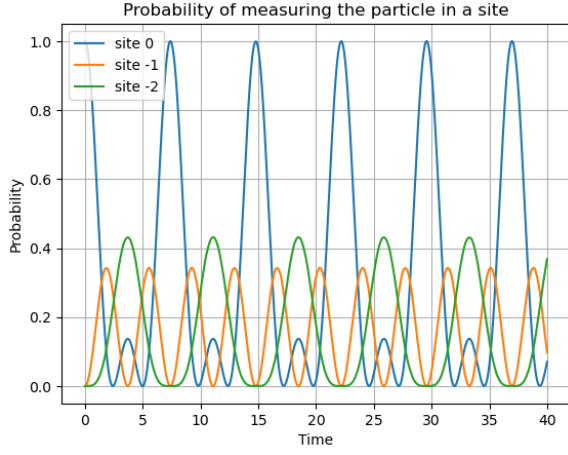


**Figure 1:** With  $\hat{H}(t)$ , the probabilities of measuring the wave function in a particular site are depicted in the high-frequency regime

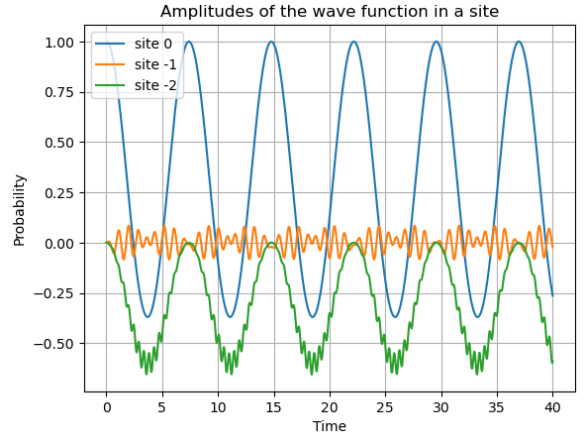


**Figure 2:** With  $\hat{H}(t)$ , the amplitudes of the wave function in a particular site are depicted in the high-frequency regime

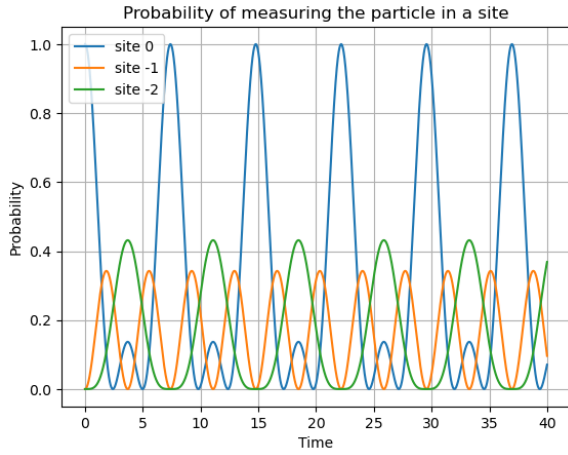


**Figure 3:** With  $\hat{H}_{eff}$ , the probabilities of measuring the wave function in a particular site are depicted in the high-frequency regime

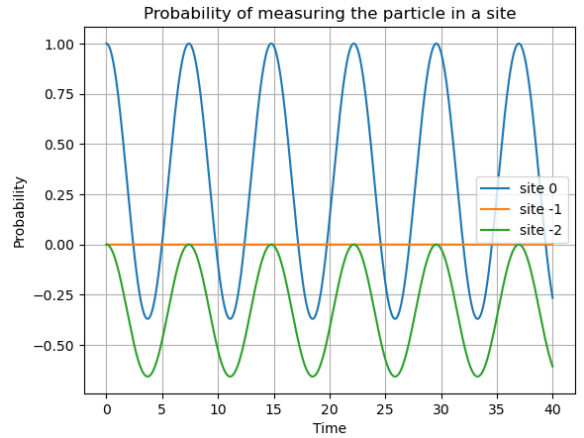


**Figure 4:** With  $\hat{H}_{eff}$ , the amplitudes of the wave function in a particular site are depicted in the high-frequency regime

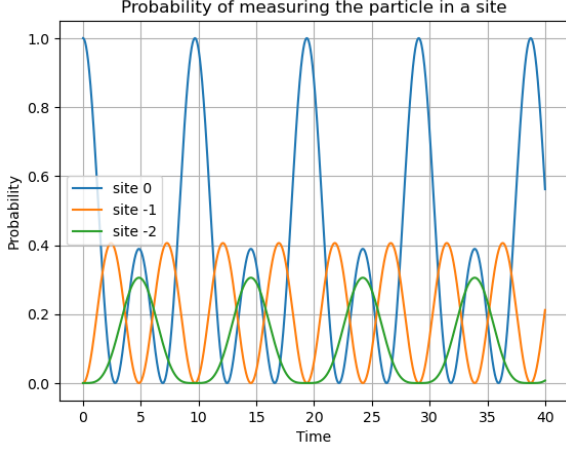


**Figure 7:** With  $\hat{H}_{eff}$ , the probabilities of measuring the wave function in a particular site are depicted in the low-frequency regime

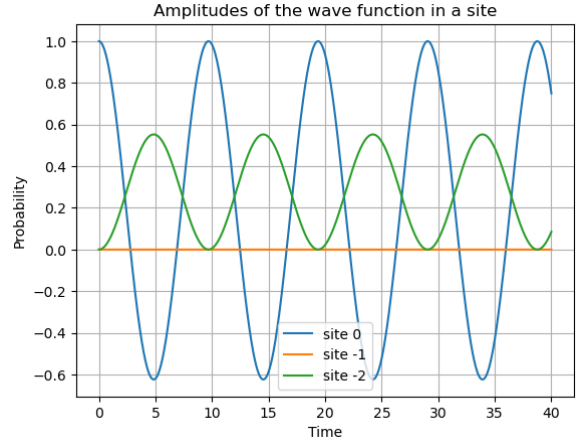


**Figure 8:** With  $\hat{H}_{eff}$ , the amplitudes of the wave function in a particular site are depicted in the low-frequency regime

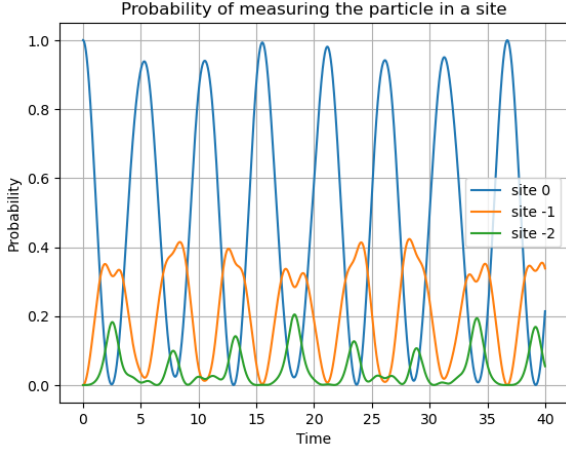


**Figure 5:** With  $\hat{H}(t)$ , the probabilities of measuring the wave function in a particular site are depicted in the low-frequency regime

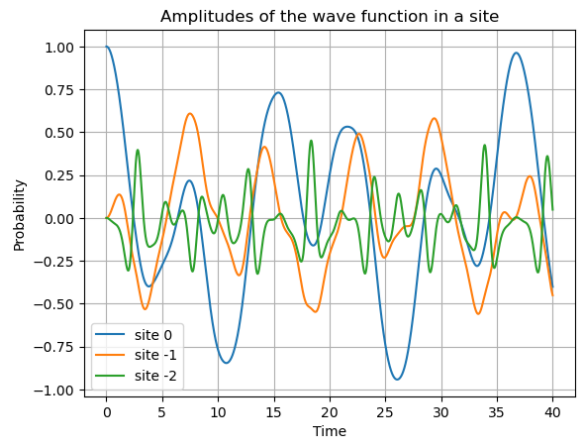


**Figure 6:** With  $\hat{H}(t)$ , the amplitudes of the wave function in a particular site are depicted in the low-frequency regime

For both  $\hat{H}(t)$  and  $\hat{H}_{eff}$  the probabilities of measuring the particle in site 0, 1 and 2 are depicted over time in Figures 5 and 7 respectively, while Figures 6 and 8 are a schematic of the correspondent amplitudes. As it can be seen, in the low-frequency regime the agreement between the two time evolutions stops: the micromotion effect emerges in the time-dependent hamiltonian and it is no more negligible.

With this simulation even if using a small number of sites in the lattice we can conclude that  $\hat{H}_{eff}$  is correctly described by formula 6, since it provides the same dynamics as  $\hat{H}(t)$  only in the high-frequency regime.

After having proved the accuracy of the effective Hamiltonian, it is possible to discuss the transition to the continuum case: we expect that this discrete Hamiltonian will behave similarly to the Hamiltonian in Eq.4. Nevertheless, approaching this problem is difficult, because we have to find the continuous limit of the discrete model where there is position-dependent tunneling: this complicates a lot our system, so some assumptions are necessary.

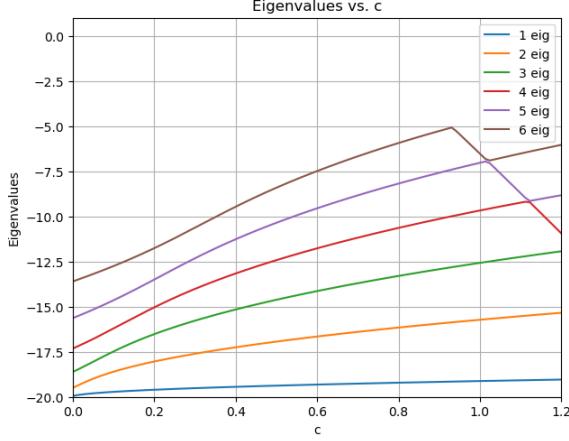


**Figure 9:** First 6 eigenvalues obtained via diagonalization of  $\hat{H}_{eff}$  as a function of  $c$

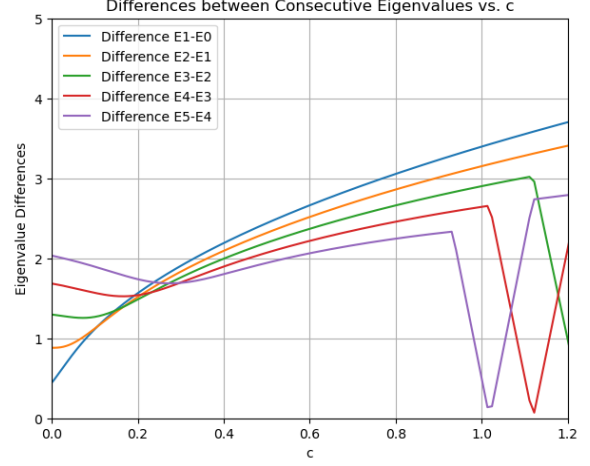


**Figure 10:** Differences between the first 6 eigenvalues of  $\hat{H}_{eff}$  as a function of  $c$

Now, one assumption that can be done is that the spectrum for a very centered wave packet at a fixed  $k$  is given by the same equation, only with a  $J(i)$  depending on the position:

$$E(k) = -2J(i) \cos(k) \quad (9)$$

The analytical derivation of this energy from the discrete Hamiltonian is complicated. Nevertheless it's possible to compare the expected behaviour for this particular energy and use numerical simulation to see if the discrete Hamiltonian in Eq.(6) is consistent with this spectrum.

If we now consider small energies ( $k \simeq 0$ ), we can expand the  $\cos(k)$  in Eq.(9): it's clear that a second order expansion will yield the Hamiltonian of a harmonic oscillator, which spectrum is described by equally spaced eigenvalues.

On the other hand the discrete Hamiltonian can be rewritten it in order to highlight a parameter  $c$  which describes how fast does the coupling change over position:

$$\hat{H}_{eff} = -J \sum_i (1 + c(2i+1)^2) (|i+1\rangle \langle i| + |i\rangle \langle i+1|) \quad \text{with } c = -\frac{V^2}{4\omega^2} \quad (10)$$

The expected behaviour is that for a specific range of the parameter  $c$  the spectrum of the discrete Hamiltonian will be made of equally spaced eigenvalues, which is enough to state that for that range we have the same behaviour of an harmonic oscillator. It is obvious that for  $c = 0$  we don't have any potential so we expect to find the bands of the unperturbed tunneling Hamiltonian (and in particular a quadratic behaviour for small  $k$ ).

Therefore, using  $N = 20$ , the first 6 different eigenvalues are depicted in Figure 9 over the value of  $c$ , while the differences between the eigenvalues over  $c$  are shown in Figure 10.

As is it possible to see, when  $c = 0$  the distance between the eigenvalues increases (quadratically) while when  $c > 1$  the eigenvalues behaves in an unexpected and strange way. In the middle, especially in the range  $[0.2, 0.4]$  the difference is quite constant and so we can approximate this range to the one in which we have equally spaced eigenvalues; this is the range in which the behaviour of our system resembles an harmonic oscillator, obtaining an agreement with the spectrum in the continuum regime.

As a matter of fact, considering different values in the correspondent range for  $V$  one gets a parabolic behaviour of the eigenvalues when  $V = 0$  and a messed up spectrum when  $V = 0.5$ , while a linear trend emerges if the correct value of  $V = 0.3$  is chosen (Figure 11).

This is true at least for the first eigenvalues; however if one starts considering higher eigenvalues

of the spectrum it is possible to notice the presence of noise that makes the spacing between consecutive eigenvalues different even in the correct range of  $c$ , as seen in Figure 10. This behaviour is also confirmed in Figure 11: the linear dependency starts to slightly break down considering higher eigenvalues.

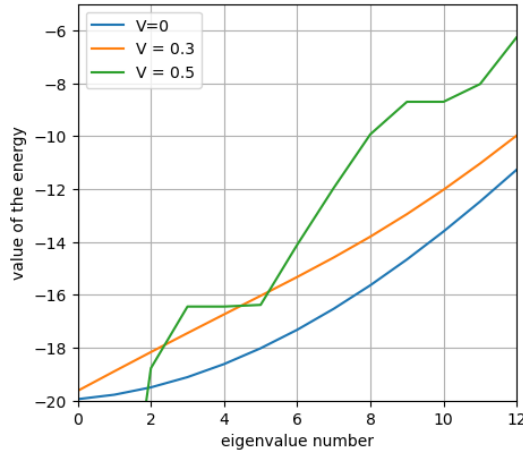


Figure 11:

## 4 Question 4

Let's now study the dynamics of a small gaussian wavepacket slightly displaced from the center of  $\hat{H}_{eff}$ .

We considered a lattice with 41 sites ( $N = 20$ ) and as wave function a Gaussian with  $\mu = 0.5$  and  $\sigma = 5$ . The gaussian wavepacket is evolved via the unitary operator defined for  $\hat{H}_{eff}$ , while the lattice parameters used in this simulation are:  $J = 10$ ,  $V = 0.3$  (which corresponds to the best value found in Question 3) and  $\omega = 9$  (we must consider the high-frequency regime).

As requested, let's focus our attention on the probability of the wave function in the center  $i = 0$  of the lattice, which is displayed in Figure 12, while in Figure 13 is depicted the time evolution of the gaussian wavepacket over the number of the site.

The behaviour of the probability over time shows an oscillation that emerges when considering a slight displacement from the origin. Doing a fit with a sinusoidal function, we obtain a value for the oscillation frequency of  $f = 0.292$  Hz, which corresponds to a period  $T = 3.422$  s.

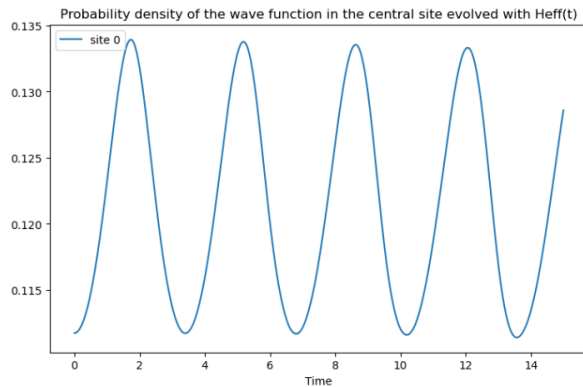


Figure 12: Time evolution of the probability  $c_0$  of the gaussian wavepacket in the site  $i = 0$  of the lattice, using  $\hat{H}_{eff}$

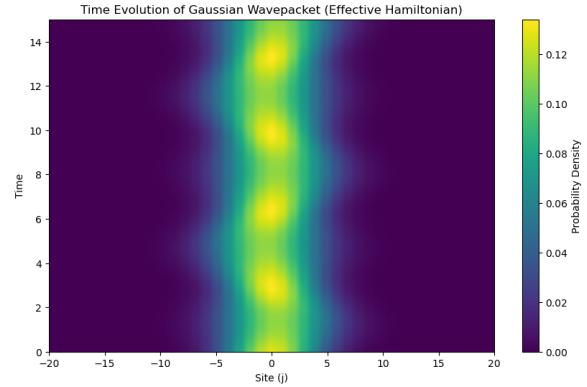


Figure 13: Time evolution of the probability  $c_0$  of the gaussian wavepacket over the sites of the lattice, using  $\hat{H}_{eff}$



It's difficult to verify that the frequency of the oscillations is the expected one. One should consider what's the quadratic term in the potential of the lattice near the origin, and from this calculate the frequency, thus the period of oscillations. Looking at Eq.(6) one in a first approximation can consider the frequency of the oscillations as defined in natural units by  $\Omega^2 = \frac{JV^2}{2\omega^2}$ , where the factor  $\frac{1}{2}$  of the quadratic potential has been removed. In this way one gets:

$$\Omega = 0.236s^{-1} \longrightarrow T = 4.24s$$

which is a bit different from the one obtained from the fit; this is due to the fact that the frequency we are considering is not the correct one because our term is not a potential but a kinetic term.

## 5 Question 5

Now let's repeat the dynamics of the previous point using the full Hamiltonian  $\hat{H}(t)$  in order to show that there is agreement with the one obtained using the effective Hamiltonian in the high-frequency regime.

The same lattice with  $N = 20$  and the same gaussian wavepacket are considered. The same parameters  $J = 10$ ,  $V = 0.3$  and  $\omega = 9$  are used, together with the correct time evolution operator for the time-dependent hamiltonian.

The time evolution of the probability of the wave function in the center  $i = 0$  is analyzed, and depicted in Figure 16, while in Figure 17 is depicted the time evolution of the probability of the gaussian wavepacket over the number of the site.

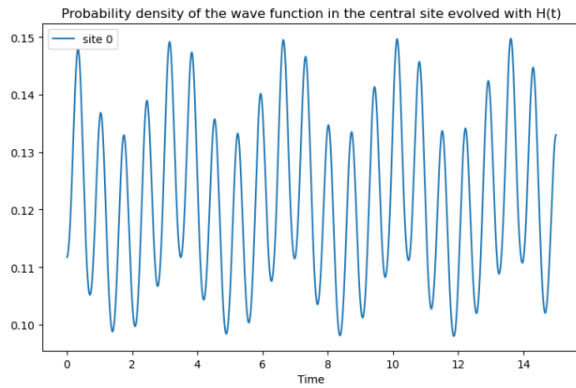


**Figure 14:** Time evolution of the probability  $c_0$  of the gaussian wavepacket in the site  $i = 0$  of the lattice, using  $\hat{H}(t)$



**Figure 15:** Time evolution of the probability  $c_0$  of the gaussian wavepacket over the sites of the lattice, using  $\hat{H}(t)$

The fit on this curve yields a frequency of the oscillations of  $f = 0.291$  Hz, with a corresponding period of  $T = 3.412$  s. Therefore, the behaviour of the probability seems to agree with the one obtained in the previous point with  $\hat{H}_{eff}$ : the oscillations have comparable frequencies, and the behaviours depicted look quite similar. However, it is possible to notice the presence of noise for  $\hat{H}(t)$  probably due to the presence of the micromotion that affects the width of the amplitude.

## 6 Question 6

Let's discuss the regime where the second order approximation breaks down. As previously said, the effective hamiltonian  $\hat{H}_{eff}$  is derived under the high-frequency regime.

For this reason let's run the simulation initializing the same gaussian wavepacket for both  $\hat{H}(t)$

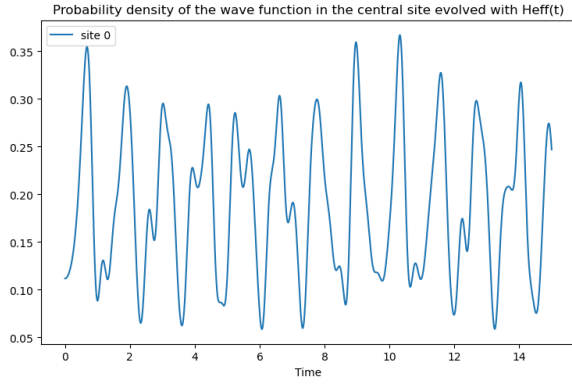


**Figure 16:** With  $\hat{H}_{eff}$ , time evolution of the probability  $c_0$  of the gaussian wavepacket in the site  $i = 0$  of the lattice,  $\omega = 3$

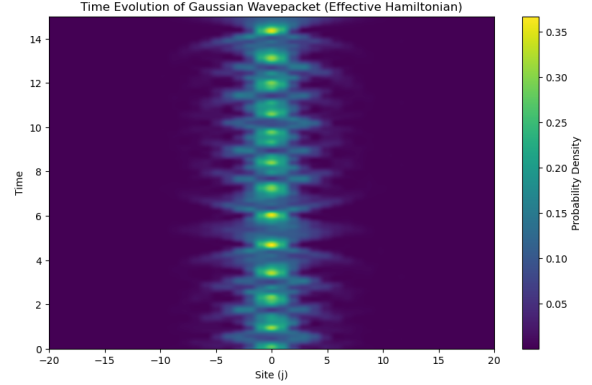


**Figure 17:** With  $\hat{H}_{eff}$ , time evolution of the probability  $c_0$  of the gaussian wavepacket over the sites of the lattice, using  $\omega = 3$

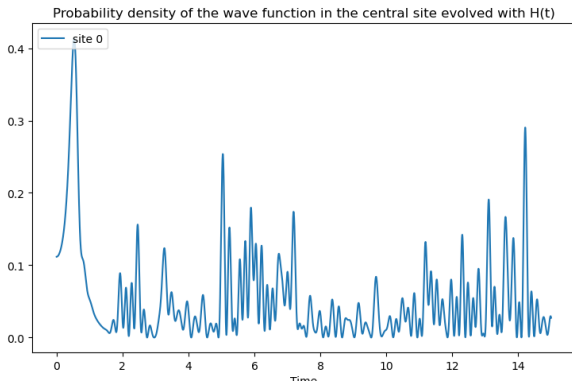


**Figure 18:** With  $\hat{H}(t)$ , time evolution of the probability  $c_0$  of the gaussian wavepacket in the site  $i = 0$  of the lattice,  $\omega = 3$

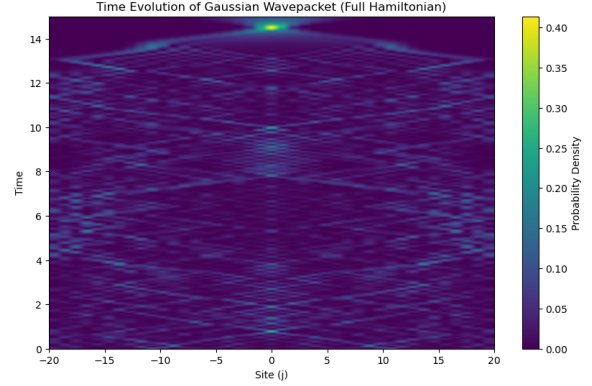


**Figure 19:** With  $\hat{H}(t)$ , time evolution of the probability  $c_0$  of the gaussian wavepacket over the sites of the lattice, using  $\omega = 3$

and  $\hat{H}_{eff}$  using a low frequency.

The results for  $\hat{H}_{eff}$  are depicted in Figure 16 and 17, where  $J = 10$ ,  $V = 0.3$  and  $\omega = 3$  are used.

On the other hand the results for  $\hat{H}(t)$  are depicted in Figure 18 and 19, where the same parameters have been used.

It is clearly evident that the second order approximation breaks down in the low-frequency regime, since the micromotion dynamics starts to emerge in  $\hat{H}(t)$ .

However it is also expected that the approximation breaks down in the high frequency regime in the case of a strong drive  $V$ . This is due to the fact that looking at the equation that describes the effective hamiltonian, the ratio  $\frac{JV^2}{4\omega^2}$  is no more small, and the higher order terms are not negligible anymore.

For this reason the simulation with the same wavepacket is run for both  $\hat{H}(t)$  and  $\hat{H}_{eff}$  by only changing the parameters of the lattice to  $J = 10$ ,  $V = 30$  and  $\omega = 9$ . The results are depicted in Figures 20 21 22 and 23 that clearly confirm the previous considerations.

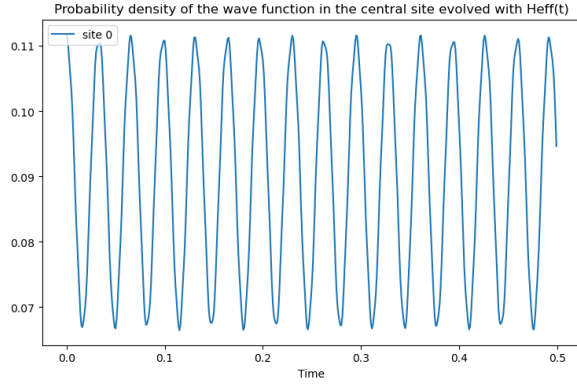


**Figure 20:** With  $\hat{H}_{eff}$ , time evolution of the probability  $c_0$  of the gaussian wavepacket in the site  $i = 0$  of the lattice,  $V = 30$

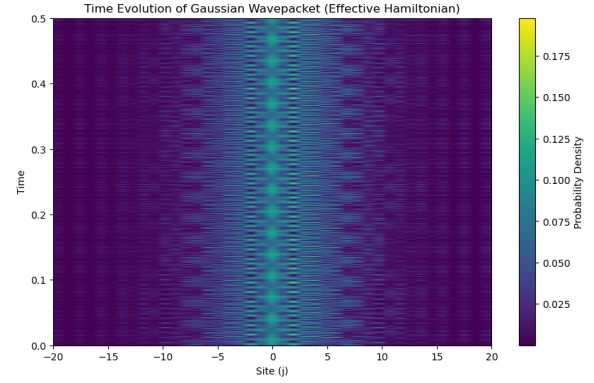


**Figure 21:** With  $\hat{H}_{eff}$ , time evolution of the probability  $c_0$  of the gaussian wavepacket over the sites of the lattice, using  $V = 30$

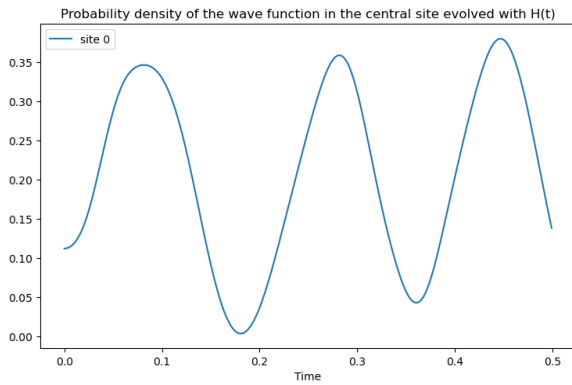


**Figure 22:** With  $\hat{H}(t)$ , time evolution of the probability  $c_0$  of the gaussian wavepacket in the site  $i = 0$  of the lattice,  $V = 30$

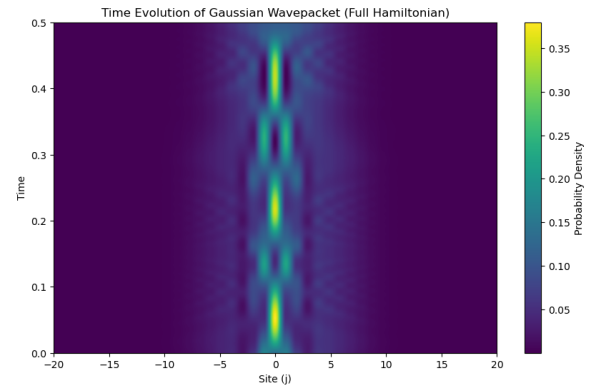


**Figure 23:** With  $\hat{H}_{eff}$ , time evolution of the probability  $c_0$  of the gaussian wavepacket over the sites of the lattice, using  $V = 30$

## A Appendix

### A.1 Commutator relations

- $[\hat{x}^2, \hat{p}^2]$ : we use the following rule to compute this commutator:

$$\begin{aligned} [\hat{A}^2, \hat{B}^2] &= \hat{A} [\hat{A}, \hat{B}^2] + [\hat{A}, \hat{B}^2] \hat{A} = \hat{A} [\hat{A}, \hat{B}] \hat{B} + \hat{A} \hat{B} [\hat{A}, \hat{B}] + [\hat{A}, \hat{B}] \hat{B} \hat{A} + \hat{B} [\hat{A}, \hat{B}] \hat{A} = \\ &= 2 [\hat{A}, \hat{B}] (\hat{A} \hat{B} + \hat{B} \hat{A}) \end{aligned}$$

Hence:

$$[\hat{x}^2, \hat{p}^2] = 2i\hbar (\hat{x}\hat{p} + \hat{p}\hat{x})$$

- $[\hat{x}\hat{p}, \hat{x}^2] + [\hat{p}\hat{x}, \hat{x}^2]$ :

$$\begin{aligned} [\hat{x}\hat{p}, \hat{x}^2] + [\hat{p}\hat{x}, \hat{x}^2] &= \hat{x} [\hat{p}, \hat{x}^2] + \cancel{[\hat{x}, \hat{x}^2]} \hat{p} + [\hat{p}, \hat{x}^2] \hat{x} + \hat{p} \cancel{[\hat{x}, \hat{x}^2]} = \\ &= -4i\hbar \hat{x}^2 \end{aligned}$$